Intrinsic Rate Constants. An interesting feature of Figure 3 is that the two Brønsted lines intersect at a point where $pK_a^{AH} + \log p/q = pK_a^{1,H^+}$, allowing a direct determination of the "intrinsic" rate constant (in the Marcus sense) for kryptopyrrole: $\log k_0 = 1.75$ at 25 °C in aqueous solution.[36] This corresponds to a relatively large intrinsic kinetic barrier, $\Delta G_0^{\ddagger} = 62.9$ kJ mol^{-1}, in agreement with the fact that the reaction destroys an aromatic ring and gives an appreciably delocalized cation. Indeed, the found intrinsic barrier is comparable to those reported for ionization of carbon acids involving extensive electronic and structural reorganization.[9,30]

From hydrogen-exchange experiments, an average value of $\Delta G_0^{\ddagger} \sim 80$ kJ mol^{-1} has been estimated for aromatic protonation.[36,37] Using the same assumption as before, i.e., $k_H/k_T \sim 18$, more comparable $\Delta G_0^{\ddagger}$ values may be estimated from reported rates of detritiation and protonation equilibrium data for azulene and 1,3,5-trimethoxybenzene.[16,17] The $\Delta G_0^{\ddagger}$ values thus obtained are both of the order of 65 kJ mol^{-1} and are then comparable to that for kryptopyrrole. This shows that the intrinsic kinetic barriers for protonation of these three structurally different aromatics are very similar.

Experimental Section

Materials. 2,4-Dimethyl-3-ethylpyrrole, i.e., kryptopyrrole (**1**), was obtained commercially (Aldrich) and twice distilled under vacuum prior to use: bp[15] 90–91 °C (lit. bp[18] 92.5–94 °C).[38]

Kryptopyrrole-5-*d*, i.e., **1**-*d*, was prepared by subjecting **1** to an acid-catalyzed exchange with D_2O, according to a procedure similar to that previously described for some indoles:[15] 1 g of **1** was dissolved in a solution consisting of 3 mL of dioxane and 3 mL of DCl (1.2 M in D_2O). This solution was allowed to stand at room temperature for 3 h and then neutralized with NaOD. After filtration and removal of the solvent, the labeled pyrrole was extracted with diethyl ether. The solution was dried over $MgSO_4$ and evaporated to yield 1,5-dideuteriokryptopyrrole (**1**-d_2) which was distilled under vacuum (yield 0.78 g). The NMR resonances of the N–H (δ 9.77 ppm) and H-5 (δ 6.25 ppm) protons of **1** in Me_2SO-d_6[39] were absent in the spectrum of **1**-d_2, but redissolution of this substrate in a water–dioxane mixture for a few minutes restored the NMR signal due to the NH group. Purification of the resulting product as described for **1**-d_2 provided a sample of **1**-*d* labeled at C-5 (>98% deuterium incorporation by NMR).

The kinetic experiments described in the Results section were carried out with **1**-*d*, but for comparison the protonation of **1**-d_2 was also studied in HCl solutions. The kinetic results obtained with **1**-d_2 were essentially the same as those obtained with **1**-*d* within the experimental errors.

Other materials (buffers) were all commercially available and were purified according to standard procedures.

Kinetic and pH Measurements. Stopped-flow determinations were performed on a Durrum stopped-flow spectrophotometer, the cell compartment of which was maintained at ±0.3 °C. All kinetic runs were carried out in triplicate under pseudo-first-order conditions with a substrate concentration of ca. 10^{-4} M. Rate constants are accurate to ±3% with the exception of some $k_{-1}^{A^-}$ and k_1^{AH} rate constants which may be to ±5%.

The pH of the buffer solutions was measured on a Tacussel Isis 20 000 electronic pH-meter according to standard methods.

Registry No. **1**, 517-22-6; **1**, H^+, 93565-19-6; **2**, 489-84-9; **4**, 30144-12-8; **5**, 930-87-0; Az-2, 941-81-1; Az-3, 93565-20-9; Az-4, 275-51-4; H_3O^+, 13968-08-6; $NCCH_2CO_2H$, 372-09-8; $ClCH_2CO_2H$, 79-11-8; $MeOCH_2CO_2H$, 625-45-6; HCO_2H, 64-18-6; CH_3CO_2H, 64-19-7; $HO_2C(CH_2)_2C(O)O^-$, 13479-42-0; $H_2PO_4^-$, 14066-20-7; H_2O, 7732-18-5; $NCCH_2C(O)O^-$, 23297-32-7; $ClCH_2C(O)O^-$, 14526-03-5; $MeOCH_2C(O)O^-$, 20758-58-1; $HC(O)O^-$, 71-47-6; $CH_3C(O)O^-$, 71-50-1; $^-OC(O)(CH_2)_2C(O)O^-$, 56-14-4; $Me_2As(O)O^-$, 15132-04-4; HPO_4^{2-}, 14066-19-4; D_2, 7782-39-0; D_3O^+, 24847-51-6; cacodylic acid, 75-60-5.

Supplementary Material Available: Observed rates of approach to equilibrium between kryptopyrrole (**1**) and its cation **1**,H^+ in aqueous solution (Table S_1), plot of $k_{obsd} - k_1^{H_3O^+}[H_3O^+]$ vs. [AH] for the cyanoacetic buffer system with $[A^-]/[AH] = 2$ (Figure S_1) (2 pages). Ordering information is given on any current masthead page.

Direct Measurement of a Prominent Outer-Sphere Electron Self-Exchange: Kinetic Parameters for the Hexaaquaruthenium(II)/(III) Couple Determined by Oxygen-17 and Ruthenium-99 NMR

Paul Bernhard,[1a,b] Lothar Helm,[1a] Andreas Ludi,[1b] and André E. Merbach*[1a]

Contribution from the Institut de Chimie Minérale et Analytique, Université de Lausanne, 3, Place du Château, CH-1005 Lausanne, Switzerland, and the Institut für Anorganische Chemie, Universität Bern, Freiestrasse 3, CH-3012 Bern, Switzerland. *Received May 30, 1984*

Abstract: The electron-exchange rate of the $Ru(H_2O)_6^{3+/2+}$ couple in acidic solutions has been measured directly by ^{17}O and ^{99}Ru NMR in the temperature range 252–366 K. The ^{17}O NMR signals for the coordinated water of $Ru(H_2O)_6^{2+}$ and $Ru(H_2O)_6^{3+}$ occur at −200 and +35 ppm vs. H_2O and the ^{99}Ru signal for $Ru(H_2O)_6^{2+}$ at +16050 ppm vs. $Ru(CN)_6^{4-}$. At high temperature the electron-exchange rate is obtained from the broadening of the NMR signals of $Ru(H_2O)_6^{2+}$ in the presence of $Ru(H_2O)_6^{3+}$. At low temperatures the exchange is followed in the ^{17}O NMR spectrum by a fast injection technique. At 298.15 K the rate constant k is 20 ± 4 M^{-1} s^{-1} and the enthalpy and entropy of activation are $\Delta H^{\ddagger} = 46.0 \pm 0.8$ kJ mol^{-1} and $\Delta S^{\ddagger} = -65.7 \pm 2.7$ J K^{-1} mol^{-1}, respectively, for a solution 2.5 M in H^+ and 5.0 M in ionic strength, the counterion being trifluoromethanesulfonate. The effect of the acid concentration and the ionic strength is discussed. From a comparison with activation parameters calculated by using solid state properties of the hexaaqua ions, a value of ≈0.01 for the electronic transmission factor $\langle\kappa\rangle_{el}$ is estimated. Among the hexaaqua ions the $Ru(H_2O)_6^{3+/2+}$ electron self-exchange represents the only unambiguous outer-sphere case since the water exchange on both hexaaqua complexes is much slower than the electron exchange.

Electron self-exchange reactions of the type

$$*ML_6^{3+} + ML_6^{2+} \underset{}{\overset{k}{\rightleftharpoons}} *ML_6^{2+} + ML_6^{3+} \qquad (1)$$

have attracted much interest as a basis for the understanding of redox reactions accompanied by a net chemical change. In spite of the simplicity of such reactions, a direct measure is by no means simple, and only a few couples have been investigated among the hexaaqua ions, i.e., $V(H_2O)_6^{3+/2+}$,[2] $Cr(H_2O)_6^{3+/2+}$,[3] $Fe(H_2O)_6^{3+/2+}$,[4] and $Co(H_2O)_6^{3+/2+}$.[5] Information about self-ex-

(1) (a) Université de Lausanne. (b) Universität Bern.

(2) Krishnamurty, K. V.; Wahl, A. C. *J. Am. Chem. Soc.* **1958**, *80*, 5292.
(3) Anderson, A.; Bonner, N. A. *J. Am. Chem. Soc.* **1954**, *76*, 3826.

0002-7863/85/1507-0312$01.50/0

Table I. Parameters for Electron Exchange and Quadrupolar Relaxation[a]

					line-width data[b]			line-width + fast injection data[c]			
soln	$[Ru^{2+}]$, M	$[Ru^{3+}]$, M	$[H^+]$, M	I, M	$\Delta H^{\ddagger}$, kJ mol^{-1}	E_Q, kJ mol^{-1}	k^{298}, M^{-1} s^{-1}	$\Delta H^{\ddagger}$, kJ mol^{-1}	k^{298}, M^{-1} s^{-1}	E_Q, kJ mol^{-1}	$1/T_{2Q}^{298}$, s^{-1}
LB1	0.152	0.703	1.80	6.47	43.1 ± 1.7	16.9 ± 0.3	25	45.9 ± 0.3	21	16.6 ± 0.2	579
LB2	0.153	0.400	1.85	4.71	43.0 ± 1.7	16.5 ± 0.3	26	45.9 ± 0.3	21	16.2 ± 0.2	486
LB3	0.149	0.407	3.76	6.65	41.5 ± 1.7	16.3 ± 0.3	48	44.3 ± 0.3	40	16.5 ± 0.2	553
Ru1	0.300	0.280	3.80	6.41		27.0 ± 1.7				25.0 ± 1.4	61
LB4	0.164	0.418	2.93	5.93	42.3 ± 1.7	16.7 ± 0.3	36	45.1 ± 0.3	29	16.4 ± 0.2	534
LB5	0.168	0.259	3.44	5.50	41.9 ± 1.7	16.5 ± 0.3	40	44.8 ± 0.3	33	16.2 ± 0.2	485
LB6	0.164	0.336	2.57	5.08	43.1 ± 1.7	16.3 ± 0.3	25	46.0 ± 0.3	20	16.0 ± 0.2	451
LB7	0.205	0.194	3.90	5.68	41.2 ± 1.7	16.5 ± 0.3	58	44.0 ± 0.3	44	16.2 ± 0.2	483

[a] Eighteen parameter fit (all standard deviations: 1σ). [b] $\Delta S^{\ddagger} = -73.52 \pm 4.68$ J K^{-1} mol^{-1}, $1/T_{2Q}^{0}(^{17}O) = 0.619 \pm 0.076$ s^{-1}, and $1/T_{2Q}^{0}(^{99}Ru) = (1.1 \pm 0.8)\ 10^{-3}$ s^{-1}. [c] $\Delta S^{\ddagger} = -65.66 \pm 0.91$ J K^{-1} mol^{-1}, $1/T_{2Q}^{0}(^{17}O) = 0.716 \pm 0.065$ s^{-1}, and $1/T_{2Q}^{0}(^{99}Ru) = (2.5 \pm 1.4)\ 10^{-3}$ s^{-1}.

change reactions can also be obtained by applying the Marcus cross relation[6] to a series of redox reactions involving the redox couple of interest; there are, however, discrepancies between directly and indirectly determined rate constants which have recently been discussed for the case of $Co(H_2O)_6^{3+/2+}$.[7] Whereas for ligands other than water, the ^1H NMR line-broadening technique is often a convenient method to study self-exchange reactions; it cannot be applied for aqua ions because the proton exchange between any $M(H_2O)_6^{n+}$ and bulk water is faster than the electron exchange. ^{17}O NMR cannot be used either in most cases because the water exchange on one (or both) aqua complex(es)[8] is faster than the electron transfer. ^{59}Co NMR has been performed on $Co(H_2O)_6^{3+}$ in the presence of $Co(H_2O)_6^{2+}$; the observed broadening, however, was due to the presence of $Co(H_2O)_5OH^{2+}$ rather than to electron exchange.[9]

An indirect value for k^{298} of 60 ± 40 M^{-1} s^{-1} has been estimated for the $Ru(H_2O)_6^{3+/2+}$ couple[10] from cross reactions. We have recently shown that this value can be rationalized by using solid-state properties of the ruthenium hexaaqua ions, i.e., force constants and bond lengths in corresponding salts.[11] Owing to the slowness of the water exchange[12] on $Ru(H_2O)_6^{2+}$ and $Ru(H_2O)_6^{3+}$, distinct ^{17}O NMR signals for the coordinated water of $Ru(H_2O)_6^{2+}$ and $Ru(H_2O)_6^{3+}$ are easily detected in ^{17}O-enriched samples, the signal for the diamagnetic $Ru(H_2O)_6^{2+}$ being narrower. A signal for $Ru(H_2O)_6^{2+}$ is also seen in the ^{99}Ru NMR spectrum. The present paper discusses the results from a study of the $Ru(H_2O)_6^{3+/2+}$ self-exchange reaction by ^{17}O and ^{99}Ru NMR in the temperature range 252–366 K, representing an unambiguous outer-sphere reaction. To our knowledge, this is the first application of ^{99}Ru NMR spectroscopy to chemical kinetics. A preliminary value for k^{298} of 44 ± 5 M^{-1} s^{-1} for a solution of 3.8 M CF_3SO_3H has been reported from line-broadening data alone.[12]

Experimental Section

A. Syntheses. Trifluoromethanesulfonic ("triflic") acid was distilled at reduced pressure (12 torr, 328 K) and ^{17}O-enriched water (32.2 atom % ^{17}O, 17.2 atom % ^{18}O, normalized in ^1H, Yeda) in vacuo before use. The triflate salts were prepared from $[Ru(H_2O)_6](tos)_2$[13] (tos = *p*-toluenesulfonate) by ion exchange under argon (elution with 1.5 M CF_3SO_3H), oxidation (for $Ru(H_2O)_6^{3+}$), and crystallization at 250 K. Both salts are hygroscopic and very soluble in H_2O, EtOH, EtOEt, and THF; the one of $Ru(H_2O)_6^{3+}$ always contained additional triflic acid and water. $[Ru(H_2O)_6](tos)_3 \cdot 3H_2O$ enriched in $H_2{}^{17}O$ (30 atom % ^{17}O)[14] was prepared by heating $[Ru(H_2O)_6](tos)_3 \cdot 3H_2O$[13] in $H_2{}^{17}O$ (32 atom % ^{17}O) containing 2 M Htos to 340 K for 3 h and isolating as described. Anal. Calcd (found) for $[Ru(H_2O)_6](CF_3SO_3)_2$: Ru, 19.92 (20.0); C, 4.74 (4.97); H, 2.38 (2.42); F, 22.47 (23.76); H_2O, 21.31 (20.99). Anal. Calcd (found) for $[Ru(H_2O)_6](CF_3SO_3)_3 \cdot 4.8H_2O \cdot 2.56CF_3SO_3H$: Ru, 8.97 (8.94); C, 5.93 (5.92); H, 2.14 (2.19); F, 28.10 (28.32); S, 15.83 (15.84); H_2O, 17.25 (14.33). Anal. Calcd (found) for $[Ru(H_2{}^*O)_6](tos)_3 \cdot 3H_2{}^*O$: Ru, 12.91 (12.8); C, 32.22 (32.7); H, 5.02 (5.1); S, 12.28 (12.0); H_2O, 21.48 (19.0). $Ru(H_2O)_6^{2+}$ and $Ru(H_2O)_6^{3+}$ were analyzed spectrophotometrically.[15] Elemental analyses were performed by Ciba-Geigy, Basle.

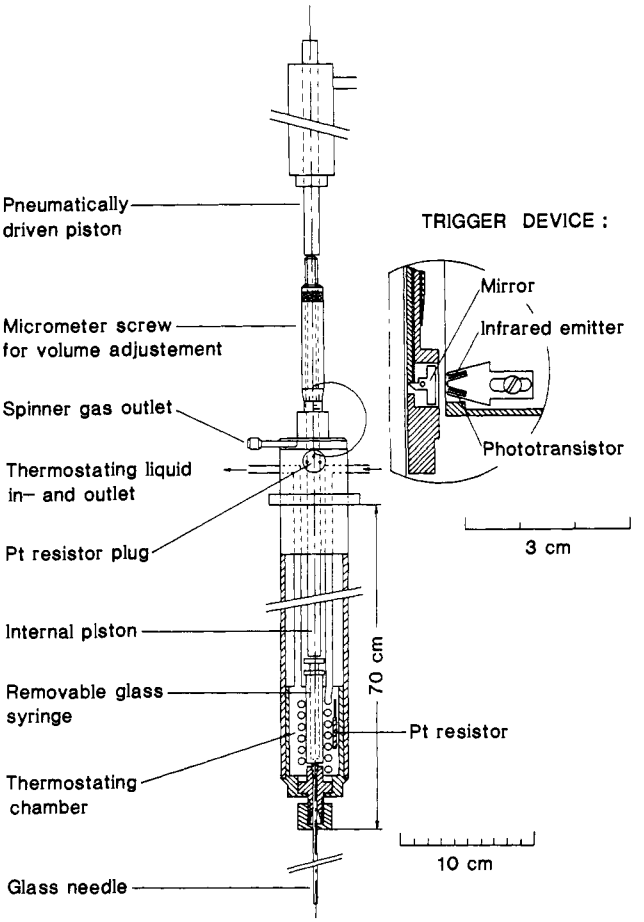

Figure 1. Schematic drawing of the insert built for fast-injection experiments.

B. Samples for NMR Measurements. Solutions for line-broadening measurements were prepared by dissolving known amounts of the triflate salts in acidified (CF_3SO_3H) oxygen-free water (for ^{17}O NMR: enriched in ^{17}O). Solution volumes were 1.20 mL. For the fast injection exper-

(4) Silverman, J.; Dodson, R. W. *J. Phys. Chem.* **1952**, *56*, 846. Brunschwig, B. S.; Creutz, C.; Macartney, D. H.; Sham, T.-K.; Sutin, N. *Faraday Disscus. Chem. Soc.* **1982**, *74*, 113. Hupp, J. T.; Weaver, M. J. *Inorg. Chem.* **1983**, *22*, 2557.
(5) Habib, H.; Hunt, J. P. *J. Am. Chem. Soc.* **1966**, *88*, 1668.
(6) Marcus, R. A. *J. Phys. Chem.* **1963**, *67*, 853.
(7) Endicott, J. F.; Durham, B.; Kumar, K. *Inorg. Chem.* **1982**, *21*, 2437.
(8) Ducommun, Y.; Newman, K. E.; Merbach, A. E. *Inorg. Chem.* **1980**, *19*, 3696. Grant, M.; Jordan, R. B. *Ibid.* **1981**, *20*, 55. Ducommun, Y.; Zbinden, D.; Merbach, A. E. *Helv. Chim. Acta* **1982**, *65*, 1386.
(9) Navon, G. *J. Phys. Chem. Lett.* **1981**, *85*, 3547.
(10) Böttcher, W.; Brown, G. M.; Sutin, N. *Inorg. Chem.* **1979**, *18*, 1447.
(11) Bernhard, P.; Ludi, A. *Inorg. Chem.* **1984**, *23*, 870.
(12) Bernhard, P.; Helm, L.; Rapaport, I.; Ludi, A.; Merbach, A. E. *J. Chem. Soc., Chem. Commun.* **1984**, 302.
(13) Bernhard, P.; Bürgi, H. B.; Hauser, J.; Lehmann, H.; Ludi, A. *Inorg. Chem.* **1982**, *21*, 3936.
(14) Throughout this paper $H_2{}^*O$ means enriched in $H_2{}^{17}O$.
(15) Bernhard, P.; Lehmann, H.; Ludi, A. *J. Chem. Soc., Chem. Commun.* **1981**, 1216.

iments (vide infra) separate solutions of $[Ru(H_2O)_6](CF_3SO_3)_2$ and $[Ru(H_2{}^*O)_6](tos)_3{\cdot}3H_2{}^*O$ in acidified (CF_3SO_3H) water were prepared. The compositions of all solutions used are given in Table I. All concentrations are given in moles per decimeters cubed at ambient temperature; no volume corrections at higher (or lower) temperatures were made.[16]

C. NMR Measurements. All the line-broadening and fast injection measurements were performed without lock on a Bruker CXP-200 spectrometer equipped with a 4.7-T Bruker wide bore superconducting magnet operating at 27.12 and 9.23 MHz for ^{17}O and ^{99}Ru, respectively. The samples were measured in 10-mm spinning tubes. The temperature was controlled by a Bruker B-VT 1000 temperature controller unit and measured before and after spectral accumulation to ±0.3 K by a substitution technique using a Pt resistance.[17] For the line-width measurements, the properly phased Fourier-transformed spectra were fitted to single Lorentzian functions, the transverse relaxation rate $1/T_2$ being obtained from the full width at half height ($\pi\Delta\nu_{1/2}$). The pulse width for $^{17}O(^{99}Ru)$ was 20 μs (42 μs), the sweep 15 000–30 000 Hz (10 000 Hz), the scan repetition time 0.035–0.104 s (0.12 s), the delay time (between the end of the pulse and the accumulation) 50 μs (500 μs), and the number of scans 1000–5000 (10 000–50 000).

For the fast injection experiments we built an apparatus which allows rapid injection of a maximum of 1 mL of a thermostated solution into a second thermostated solution contained in a commercial NMR tube. This apparatus (Figure 1) fits into the upper part of the bore (50-mm effective diameter) of our superconducting magnet. By means of a flange, the apparatus is set on a heavy brass ring placed on the top of the magnet and designed to absorb the shock due to the gas-propelled injection. The pneumatically driven piston and the trigger device are also fixed onto this ring.

A pneumatically driven piston operating at 0.8 MPa pushes the internal piston and the syringe piston. The path length of the internal piston is set by a micrometer screw, allowing the injection of volumes of up to 1 mL with a precision of 10 μL. The injection apparatus is coupled with a trigger device. The piston displacement causes rotation of a mirror into a vertical position, and the consequent reflection of infrared radiation from an emitter onto a phototransistor triggers spectral acquisition. The removable glass syringe (Hamilton Co.) is screwed into the bottom of the thermostating chamber through which is pumped a thermostating liquid. The temperature is measured by means of a platinum resistor (Heraeus, Pt 100-Ω GS 1218). The needles, easy to replace, are glass capillaries of 0.4-mm internal diameter (0.7-mm external diameter) and 115 mm in length and fit into the center of 5 or 10 mm diameter commercial NMR tubes shortened to 150 mm. Rotation and thermostatization of the tube are carried out by using the inbuilt spectrometer facilities. About 5 min is needed between experiments, mainly to change and refill the syringe. Thermal equilibration of the solution in the syringe is achieved within 15 min even for extreme temperatures (220 or 370 K). The mixing time of two 1-mL solutions in a 10-mm spinning tube is less than 50 ms.

In all the experiments 0.80 mL of a $Ru(H_2O)_6{}^{2+}$ solution was added to 0.80 mL of a solution containing $[Ru(H_2{}^*O)_6](tos)_3{\cdot}3H_2{}^*O$, and the increase in intensity (=signal height) of the $Ru(H_2{}^*O)_6{}^{2+}$ signal was followed in an automatic sequence. The pulse width was 50 μs, the sweep 13 500 MHz, the scan repitition time 0.011–0.020 s, the delay time 50 μs, the number of scans for one spectrum 700–1400, the accumulation time 12–25 s, and the exponential multiplication factor (line broadening) 100–200 Hz.

D. Data Treatment. All calculations and fits were performed on a NORSK ND 560 and ND 100 computer (Lausanne) and IBM 3033 computer (Bern) using standard least-squares programs.

Theoretical Section

A. Line-Broadening Measurements. In the limit of slow exchange[18] the transverse relaxation rate $1/T_2$ of ^{17}O and ^{99}Ru for the diamagnetic $Ru(H_2O)_6{}^{2+}$ in the presence of $Ru(H_2O)_6{}^{3+}$ is given by the sum (eq 2) of the quadrupolar relaxation and the electron exchange rate

$$1/T_2 = 1/T_{2Q} + 1/\tau \tag{2}$$

where τ is the electron-exchange lifetime expressed by

$$1/\tau = -\frac{d[Ru(H_2O)_6{}^{2+}]}{[Ru(H_2O)_6{}^{2+}]dt} = k[Ru(H_2O)_6{}^{3+}] \tag{3a}$$

$$k = (k_B T/h)\exp(\Delta S^{\ddagger}/R - \Delta H^{\ddagger}/RT) \tag{3b}$$

Equations 4 and 5 describe the quadrupolar ^{17}O relaxation rate in $Ru(H_2O)_6{}^{2+}$.[19] I, Q, χ, and η are the spin quantum number,

$$1/T_{2Q} = \frac{3\pi^2}{10}\frac{2I+3}{I^2(2I-1)}\chi^2(1+\eta^2/3)\tau_c \tag{4}$$

$$\chi = \frac{e^2 q_{zz} Q}{h} \tag{5a}$$

$$\eta = \frac{q_{yy} - q_{xx}}{q_{zz}} \tag{5b}$$

the electric quadrupole moment of the nucleus, the quadrupole coupling constant, and the asymmetry parameter of the electric field gradient tensor, respectively, its largest eigenvalue being q_{zz}. τ_c, a reorientational correlation time is usually well represented by an Arrhenius-type function[20] (eq 6) where

$$\tau_c = \tau_c{}^{\circ}\exp(E_Q/RT) \tag{6}$$

E_Q is an activation energy for the reorientation. Equation 4 can be written as

$$1/T_{2Q} = (1/T_{2Q}{}^{\circ})\exp(E_Q/RT) \tag{7}$$

For ^{99}Ru in the highly symmetric environment of $Ru(H_2O)_6{}^{2+}$, eq 4 does not apply (see Results section C). Nevertheless, eq 7 can be used to describe empirically the temperature dependence of T_{2Q} of ^{99}Ru. A plot of $\ln(1/T_2)$ vs. $1/T$ gives, thus, two limiting straight lines with slopes of E_Q/R and $-\Delta H^{\ddagger}/R$.

B. Fast Injection Experiments. The concentration of $Ru(H_2{}^*O)_6{}^{2+}$ after mixing the solutions of $Ru(H_2O)_6{}^{2+}$ and $Ru(H_2{}^*O)_6{}^{3+}$ is described by the McKay relation (eq 8) where $[Ru(H_2{}^*O)_6{}^{2+}]_{eq}$ and ΣRu are the equilibrium concentration of $Ru(H_2{}^*O)_6{}^{2+}$ and the total concentration of Ru(II) and Ru(III), respectively.

$$[Ru(H_2{}^*O)_6{}^{2+}](t) = [Ru(H_2{}^*O)_6{}^{2+}]_{eq}(1 - \exp(-kt\Sigma Ru)) \tag{8}$$

The observed NMR intensity I_n of the $Ru(H_2{}^*O)_6{}^{2+}$ signal is given by eq 9[21] where t_n and T_0 are the half-time of the nth accumulation and the accumulation time, respectively.

$$I_n(t) = I_{eq}\left(1 - \frac{2\sinh(kT_0\Sigma Ru/2)}{kT_0\Sigma Ru}\exp(-kt_n\Sigma Ru)\right) \tag{9}$$

Results

A. Chemical Shifts; Relative Rates of Water and Electron Exchange. Figure 2 shows the changes in the ^{17}O NMR spectrum at 288 K after the addtion of $[Ru(H_2O)_6](CF_3SO_3)_2$ to a solution of $[Ru(H_2{}^*O)_6](tos)_3{\cdot}3H_2{}^*O$ in acidified (CF_3SO_3H) water. The signals of $Ru(H_2{}^*O)_6{}^{3+}$ (a), $H_2{}^*O$ (b), and $Ru(H_2{}^*O)_6{}^{2+}$ (c) occur at +35, ≈0, and −198 ppm vs. acidified $H_2{}^*O$, respectively. The relative rates of the water and electron exchange are nicely illustrated. Before $Ru(H_2O)_6{}^{2+}$ is added ($t < 0$) no decrease of the $Ru(H_2{}^*O)_6{}^{3+}$ signal is observed.[22] After the addition the signal of $Ru(H_2{}^*O)_6{}^{2+}$ develops due to rapid electronic equilibration between $Ru(H_2O)_6{}^{2+}$ and $Ru(H_2{}^*O)_6{}^{3+}$. Both signals then start to decrease simultaneously due to the water exchange on

(16) Molarities rather than molalities which are frequently used in NMR were chosen because of the high concentration of triflic acid and the high ionic strength in our samples and for the purpose of comparison with the literature where all bimolecular rate constants are given in $dm^3\ mol^{-1}\ s^{-1}$.

(17) Ammann, C.; Meier, P.; Merbach, A. E. *J. Magn. Reson.* **1982**, *46*, 319.

(18) Martin, M. L.; Martin, G. J.; Delpuech, J.-J. "Practical NMR Spectroscopy"; Heyden & Son Ltd.: London, 1980; p 300.

(19) Abragam, A. "The Principles of Nuclear Magnetism"; Oxford University Press: London, 1961; p 309.

(20) Bloembergen, N. *J. Chem. Phys.* **1957**, *27*, 572, 595.

(21) Equation 9 is obtained from the integration of eq 8. The well-known simplification $2\sinh(kT_0\Sigma Ru/2)/(kT_0\Sigma Ru) = 1$ cannot be made since the condition $T_0 \ll 1/(k\Sigma Ru)$ is not fulfilled.

(22) The signal is broader than the one of $Ru(H_2O)_6{}^{2+}$ by a factor of about 5; in addition to the quadrupolar relaxation there are contributions to the line width from the hyperfine and dipole–dipole interactions with the electron spin.

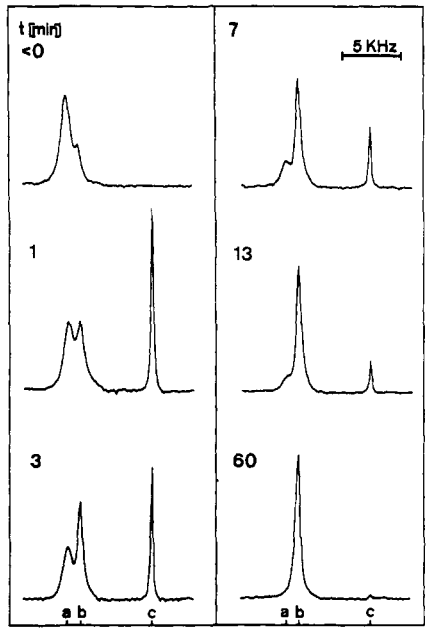

Figure 2. ^{17}O NMR spectra, 27.12 MHz, at 288 K after the addition ($t = 0$) of $Ru(H_2O)_6(CF_3SO_3)_2$ to a solution of $Ru(H_2{}^*O)_6(tos)_3{\cdot}3H_2{}^*O$ with the signals of $Ru(H_2{}^*O)_6^{3+}$ (a), $H_2{}^*O$ (b), and $Ru(H_2{}^*O)_6^{2+}$ (c) at +35, 0, and −198 ppm vs. $H_2{}^*O$.

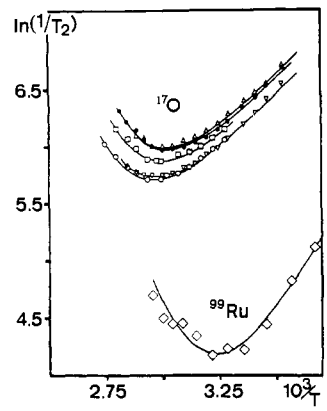

Figure 3. Plot of ln $(1/T_2)$ of $Ru(H_2O)_6^{2+}$ vs. $1/T$ in the presence of $Ru(H_2O)_6^{3+}$ for solutions LB1 (△), LB2 (▽), LB3 (●), LB4 (□), LB5 (○) (^{17}O), and Ru1 (◇) (^{99}Ru).

$Ru(H_2{}^*O)_6^{2+}$ whereas the bulk signal increases.[23] $Ru(H_2O)_6^{3+/2+}$ is thus so far the only hexaaqua redox couple where the water exchange on both complexes is slower than the electron exchange.[12]

A chemical shift scale of ^{99}Ru has recently been published.[24] We detected the signal for $Ru(H_2O)_6^{2+}$ at +16050 ppm vs. $Ru(CN)_6^{4-}$ which represents the highest frequency so far observed for a ruthenium compound.

B. Relaxation of $Ru(H_2O)_6^{2+}$ and Fast-Injection Experiments. Figures 3 and 4 show the transverse relaxation rates $1/T_2$ of $Ru(H_2O)_6^{2+}$ as a function of reciprocal temperature for solutions LB1–LB7 and Ru1 (Table I). At the low temperatures $1/T_2$ is governed by quadrupolar relaxation only, at 335 (315) K the ^{17}O (^{99}Ru) signal starts to broaden due to electron transfer,[25] and at the high temperatures $1/T_2$ is more than 70% governed by electron exchange. However, even if the rates of the electron-transfer

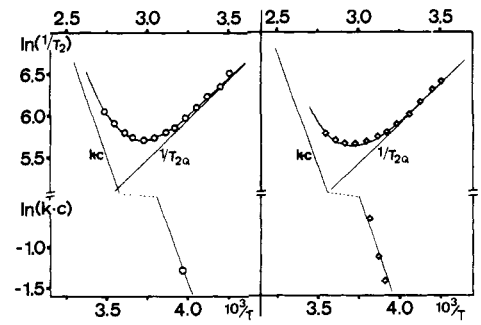

Figure 4. Plot of ln $(1/T_2(^{17}O))$ of $Ru(H_2O)_6^{2+}$ vs. $1/T$ in the presence of $Ru(H_2O)_6^{3+}$ for solutions LB6 (◇) and LB7 (○) (upper points) and fast-injection data (lower points) with the limiting straight lines for the electron exchange and the quadrupolar relaxation.

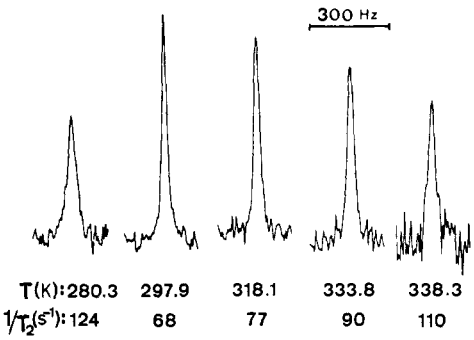

Figure 5. ^{99}Ru NMR signal, 9.23 MHz, of $Ru(H_2O)_6^{2+}$ in the presence of $Ru(H_2O)_6^{3+}$ (solution Ru1) at various temperatures.

process are well defined at the high temperatures, it is not possible to refine the four parameters $1/T_{2Q}{}^0$, E_Q, ΔS^* (or k^{298}), and ΔH^* independently for each solution because of the rather limited temperature range where the electron transfer contributes appreciably to the line width. It is also apparent from the data that the relaxation rates do not only vary with the observed nuclei but also with sample composition. Therefore, the problem cannot be reduced to a six parameter fit ($1/T_{2Q}{}^0$ and E_Q for both ^{17}O and ^{99}Ru, ΔS^* (or k^{298}) and ΔH^*) of the $1/T_2$ data of the eight solutions studied. However, in order to reduce the number of unknown (32 in total), we made the reasonable assumption, since our solutions are all high in ionic strength, of ΔS^* being equal for all solutions and $1/T_{2Q}{}^0$ being equal for the solutions LB1–LB7.[26] Moreover, as the solutions LB3 and Ru1 are very similar in acidity and ionic strength we assumed an identical activation enthalpy, ΔH^*.[12] This leaves us with 18 parameters to be adjusted: 2 values of $1/T_{2Q}{}^0$ (one ^{17}O and one for ^{99}Ru), 8 energies of activation (E_Q), the common activation entropy (ΔS^*), and seven activation enthalpies (ΔH^*). The possibility for E_Q and ΔH^* to vary from sample to sample reflects these different compositions. Because of the rather poor quality of the ^{99}Ru spectra (Figure 5) their weights in the least-squares fit were only small. The 18 parameters and their standard deviations obtained in fitting all line-broadening data to eq 2, 3b, and 7 as well as the k^{298} rate constants calculated from the kinetic activation parameters are given in Table I. The correlation coefficients between the kinetic activation parameters were still very large so that the precision in k^{298} is affected by the extrapolation of the well-defined high-temperature kinetic data to room temperature.

In order to improve the accuracy on the kinetic activation parameters, it was imperative to extend the temperature range of the kinetic determinations. Since it was not possible to extend the line-broadening measurements to higher temperatures,[27] we

(23) The signal is very much broadened (but not shifted) with respect to pure acidified $H_2{}^{17}O$ due to traces of Mn^{2+} originating from the solid triflate salts. The concentration of Mn^{2+} calculated from the line width (c.f. ref 8) is 5×10^{-4} M.

(24) Brevard, C.; Granger, P. *Inorg. Chem.* **1983**, *22*, 532.

(25) A plot of ln $(1/T_{2Q}(^{17}O))$ vs. $1/T$ for an acidified $Ru(H_2O)_6^{2+}$ solution was linear up to 350 K. A small deviation above 350 K was attributed to traces of $Ru(H_2O)_6^{3+}$ which are difficult to avoid at high temperature. Parameters were $1/T_{2Q}{}^0(^{17}O) = 0.90 \pm 0.14$ s^{-1}, $E_Q = 15.05 \pm 0.40$ kJ mol^{-1}, and $1/T_{2Q}{}^{289} = 392$ s^{-1}.

(26) If ΔH^* instead of ΔS^* is assumed to be the same for all solutions, the rate constants k^{298} change by less than 5%.

(27) To avoid decomposition of the samples, high acid concentrations had to be used. A high concentration of $Ru(H_2O)_6^{2+}$ was necessary to minimize the accumulation time at high temperatures; the concentration of $Ru(H_2O)_6^{3+}$ was high to make the electron-exchange contribution to $1/T_2$ large (cf. eq 3a).

Table II. Rate Constants from Fast-Injection Experiments

soln	$[Ru^{2+}]$, M	$[Ru^{3+}]$, M	$[H^+]$, M	I, M	T, K	k_{expti}, $M^{-1}\ s^{-1}$	k_{calcd}, $M^{-1}\ s^{-1}$
FI1	0.026	0.024	4.00	4.21	251.8	1.43 ± 0.12[a]	1.8[b]
FI2	0.025	0.023	2.50	2.71	255.8	0.72 ± 0.06	1.2[c]
FI2	0.025	0.023	2.50	2.71	258.5	0.96 ± 0.09	1.5[c]
FI2	0.025	0.023	2.50	2.71	261.1	1.54 ± 0.15	1.8[c]

[a] Mean value of three experiments with different accumulation parameters. [b,c] Extrapolated using $\Delta H^{\ddagger}$ and $\Delta S^{\ddagger}$ values for solutions LB7 and LB6, respectively, as obtained in the 18 parameter line-width data fitting procedure (Table I).

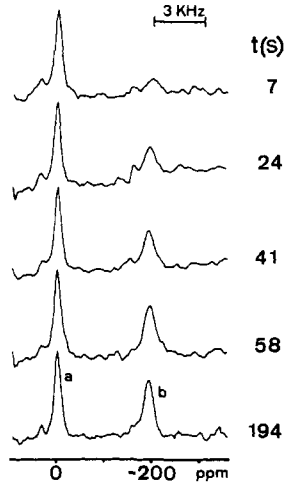

Figure 6. ^{17}O NMR spectra, 27.12 MHz, after the fast injection of a solution of $Ru(H_2O)_6(CF_3SO_3)_2$ to a solution of $Ru(H_2{}^*O)_6(tos)_3{\cdot}3H_2{}^*O$ with the signals of bulk $H_2{}^*O$ (a) and $Ru(H_2{}^*O)_6^{2+}$ (b).

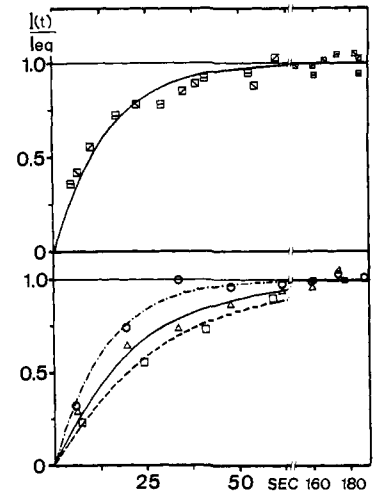

Figure 7. Intensity of the ^{17}O signal for $Ru(H_2{}^*O)_6^{2+}$ in the fast-injection experiments: upper curve, 4.0 M CF_3SO_3H, T = 251.8 K (three experiments: ⊟, ⊡, and ⊠); lower curves, 2.5 M CF_3SO_3H, T = 255.8 K (- - -), T = 258.5 K (—) and T = 261.1 K (-·-·-).

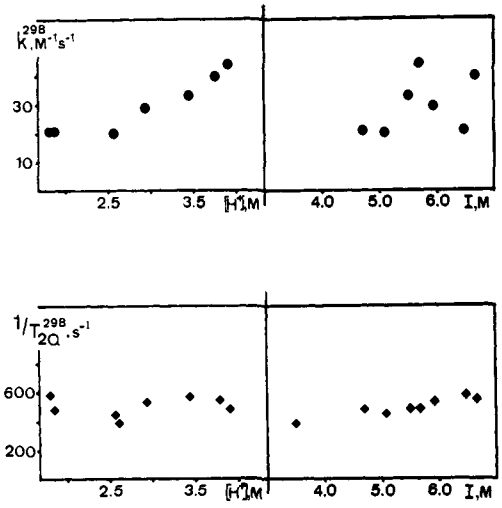

Figure 8. Plots of the electron-exchange rate constant k^{298} and of $1/T_{2Q}{}^{298}(^{17}O)$ vs. $[H^+]$ and ionic strength.

focused our efforts to follow the electron exchange at very low temperature by a fast-injection technique described in the Experimental Section. Since the reaction remained fairly rapid to be measured with this technique, a judicious choice of the concentration and of the accumulation parameters was of crucial importance. In order to compare with the line-broadening results, solutions of 4.0 and 2.5 M CF_3SO_3H were chosen (Table II). Measurements were made at 251.8 K (4.0 M CF_3SO_3H) and at 255.8, 258.5, and 261.1 K (2.5 M CF_3SO_3H). The spectra obtained at 255.8 K are shown as an example in Figure 6. The signals of bulk $H_2{}^*O$ (a) and $Ru(H_2{}^*O)_6^{2+}$ (b) are of equal intensity in equilibrium.[28] Figure 7 and Table II summarize the results of the fits of the measured intensities to eq 9 and compare them with the values obtained from the extrapolation of the line-width results of solutions LB6 and LB7 to low temperatures. Considering the large difference between the relevant temperature ranges, we observe excellent agreement between the corresponding values of k. The extrapolated values are only 20–55 % higher than the directly measured values. Moreover, the same acid dependence is found for k, i.e., an increase by a factor of about 2 going from 2.5 to 4.0 M in H^+. We, therefore, included the fast-injection kinetic data of solutions FI1 and FI2 by adding them as low-temperature values to the data set of solutions LB7 and LB6 since they are very similar in acidity. The fitting procedure was then repeated using the extended data set and using the same 18 adjustable parameters as in the first fit. The new adjusted parameters and their standard deviations as well as the calculated k^{298} values are given in Table I. The inclusion of the fast-injection data results in a drastic reduction in the computed standard deviation for the kinetic activation parameters, whereas there is only a minor improvement for the quadrupolar relaxation parameters. This excellent accuracy in the kinetic activation parameters is related to the fact that good rate constants are available for temperatures as different as 112 K. Errors as given by standard deviations are, however, underestimated. We estimate the values of k^{298}, which are now interpolated values, to be accurate to ±20%.[29] As a representative value for the electron self-exchange of the $Ru(H_2O)_6^{3+/2+}$ couple we adopt

$$k^{298}: \ 20 \pm 4\ M^{-1}\ s^{-1}$$

$$\Delta H^{\ddagger}: \ 46.0 \pm 0.8\ kJ\ mol^{-1}$$

$$\Delta S^{\ddagger}: \ -65.7 \pm 2.7\ J\ K^{-1}\ mol^{-1}$$

$$([H^+] = 2.5\ M,\ I = 5.0\ M) \qquad (10)$$

Correlations of k^{298} and $1/T_{2Q}(^{17}O)$ with $[H^+]$ and the ionic strength are shown in Figure 8. $1/T_{2Q}(^{17}O)$ shows a tendency to increase with ionic strength as a consequence of the increase

(28) This is because the bulk signal arises from the crystal water in $Ru(H_2{}^*O)_6(tos)_3{\cdot}3H_2{}^*O$ and the concentrations of Ru(II) and Ru(III) are very similar (Table II).

(29) Sources of errors are the oxidation of $Ru(H_2O)_6^{2+}$ at high temperatures, neglection of hydrolysis of $Ru(H_2O)_6^{3+}$ (the "acid-dependent path"), and the approximations made in the least-squares refinement.

in viscosity. The value obtained in the absence of $Ru(H_2O)_6^{3+}$ fits nicely into this trend.[25]

C. Parameters of Quadrupolar Relaxation. The relaxation rates of ^{99}Ru and ^{17}O are both governed by electric quadrupolar interaction caused by fluctuating electric field gradients. The correlation time τ_c for the ^{17}O relaxation is (mainly) the tumbling time for water in the first coordination sphere of the cation whereas the ^{99}Ru quadrupolar relaxation reflects the distortion of the octahedral symmetry of the complex.

An estimation of the correlation time of a bound water molecule can be made with eq 4 using the quadrupolar coupling constant (eq 5a) and the asymmetry parameter (eq 5b) for free water.[30] The correlation time of 9 ps is comparable with values ranging from 13 ps for Mg^{2+} to about 8 ps for Sr^{2+} measured by ^1H NMR in aqueous alkaline earth solutions.[31] There is also a good agreement when comparing the activation energies: 16.5 kJ mol^{-1} measured for Ru^{2+} fits well in the range of 21.6 kJ mol^{-1} for Mg^{2+} to 15.3 kJ mol^{-1} for Sr^{2+}.

A theoretical description for the ^{99}Ru relaxation rate is more difficult. Friedman[32] used crystal field theory to describe the distortion of symmetry whereas Hertz's model[33] is based on the molecular tumbling of water molecules in the first coordination sphere. Both models include the Sternheimer antishielding factor which is unknown for Ru^{2+}. Rough estimations led us to a fairly good agreement of the experimental $1/T_{2Q}^{298}$ of 60 s^{-1} and estimates of 30–300 s^{-1} for both theories if a Sternheimer factor of 20–30 is used.[34]

Discussion

Since our values of k^{298} (cf. Table I) do not correlate with the ionic strength, the latter cannot be a useful concept to describe the increase of k^{298} with increasing acid concentration. We assume that the corresponding small decrease in the activation enthalpy (2 kJ mol^{-1}) is due to a decrease (6–8%) of the outer-sphere reorganization free energy which is frequently taken as a pure reorganization enthalpy.[35] Since no dielectric constants and refraction indexes for concentrated acids are available, it is difficult to give a quantitative explanation for this effect.

For the discussion of the different contributions to the experimental activation parameters we explicitly introduce the electronic transmission factor $\langle\kappa\rangle_{el}$[36] into eq 3b:

$$k = \langle\kappa\rangle_{el} \frac{k_B T}{h} \exp(-\Delta G^*/RT) \quad (11)$$

$$\Delta G^* = w_r + \Delta G^*_{trans} + \Delta G^*_{out} + \Delta G^*_{in}(T) \quad (12)$$

In a recent review[37] expressions for the various contributions have been summarized. If we neglect the work term, w_r, in our solutions (of high ionic strength) as well as ΔS^*_{out},[35] comparison of eq 3b with eq 11 and 12 leads to the following expressions for ΔH^* and ΔS^*:

$$\Delta H^* = \Delta G^*_{out} + \Delta H^*_{in}(T) \quad (13)$$

$$\Delta S^* = R \ln \langle\kappa\rangle_{el} + R \ln \frac{Kh}{k_B T} + \Delta S^*_{in}(T) \quad (14)$$

where K is either the collision frequency Z (Marcus) or $K_A{}^0\nu_n$, the product of the Eigen–Fuoss preexponential factor and the effective nuclear frequency.[38] Nonadiabaticity is thus expected to be reflected mainly in ΔS^*.

The classical activation free energy for rearrangement of the inner coordination sphere calculated from force constants and bond length changes (17.0 kJ mol^{-1})[12] is only slightly lowered (0.6 kJ mol^{-1}) by nuclear tunneling at 298 K but "redistributed" between the activation enthalpy and entropy: $\Delta H^*_{in}(298\ K) = 13.4$ kJ mol^{-1} and $\Delta S^*_{in}(298\ K) = -10.1$ J K^{-1} mol^{-1}.[39] Introducing these values into eq 13 and 14 leads to $\Delta G^*_{out} = 32$ kJ mol^{-1} and $R(\ln \langle\kappa\rangle_{el} + \ln (Kh/k_BT)) = -55$ J K^{-1} mol^{-1}. Calculated values for ΔG^*_{out} for $Fe(H_2O)_6^{3+/2+}$ lie in the range 25–35 kJ mol^{-1}, depending upon the model used.[37] For K we use calculated values for $Fe(H_2O)_6^{3+/2+}$ (0.03–0.7) which leads to an upper and a lower limit for the electronic transmission factor for $Ru(H_2O)_6^{3+/2+}$:

$$0.03 > \langle\kappa\rangle_{el} > 0.002 \quad (15)$$

For $\langle\kappa\rangle_{el} \ll 1$ it is related to the electronic coupling matrix element H_{AB} between the corresponding wave functions of the precursor and the successor complex by[37]

$$H_{AB} = 5.58\sqrt{\langle\kappa\rangle_{el}\nu_n}\ \sqrt[4]{\Delta G^*_{in} + \Delta G^*_{out}}\ [cm^{-1}] \quad (16)$$

where ν is expressed in cm^{-1} and ΔG^* in kJ mol^{-1}. When $\Delta G^*_{out} + \Delta G^*_{in} = 50$ kJ mol^{-1} and $\nu_n = 280$ cm^{-1} are used,[38] H_{AB} becomes

$$10\ cm^{-1} < H_{AB} < 40\ cm^{-1} \quad (17)$$

Unfortunately there is no independent experimental access to the electronic coupling element H_{AB} for $Ru(H_2O)_6^{3+/2+}$. In stronger coupled systems H_{AB} can often be estimated from intervalence transitions.[40] The absorption spectrum of a solution with very high concentrations (≈1.2 M) of $Ru(H_2O)_6^{2+}$ and $Ru(H_2O)_6^{3+}$ showed, as expected, no indication of an intervalence band which should occur at 15 000–18 000 cm^{-1} in our system ($E_{op} = 4\Delta G^*$).[40]

A comparison of the $Ru(H_2O)_6^{3+/2+}$ with the $Fe(H_2O)_6^{3+/2+}$ couple is somewhat surprising. If we assume all contributions to ΔG^* except $\Delta G^*_{in}(298\ K)$ (calculated 16.4 kJ mol^{-1} for Ru[11] and 32.2 kJ mol^{-1} for Fe[37]) to be the same, the ratio $k(Ru)/k(Fe)$ is calculated to be 500. The experimental ratio is only 5.4 Moreover, the activation enthalpies, where differences in $\Delta G^*_{in}(298\ K)$ should predominantly be reflected, are very similar (46 kJ mol^{-1}). The analogous comparison between $Ru(NH_3)_6^{3+/2+}$ and $Ru(H_2O)_6^{3+/2+}$ gives an excellent agreement beteen the calculated (200) and observed (1000) ratio of the exchange rates. For this reason we assume some additional (bridging?) mechanism, lowering ΔH^*_{in} for the $Fe(H_2O)_6^{3+/2+}$ couple. The very fast water exchange[8] on $Fe(H_2O)_6^{2+}$ may be important in this context.

These comparisons together with the fact that the water exchange on both $Ru(H_2O)_6^{2+}$ and $Ru(H_2O)_6^{3+}$ is slower than the electron exchange (unique among the metal hexaaqua ions) show that the latter is a prototype of an outer-sphere electron-transfer reaction. The estimated value[10] for k^{298} from cross reactions (60 ± 40 M^{-1} s^{-1}, 1.0 M CF_3SO_3H) compares well with our directly measured value (20 ± 4 M^{-1} s^{-1}, 2.5 M CF_3SO_3H, $I = 5.0$ M). Measurements at lower ionic strength and acidity are, of course, desirable but probably very difficult because of lack of an appropriate experimental method.

Acknowledgment. We thank Dr. C. Brevard, Bruker-Spectrospin, for the help in detecting Ru NMR signals, Dr. Wagner, Ciba-Geigy AG, for the elemental analyses, a referee for constructive comments on the ^{99}Ru quadrupolar relaxation mechanism, and the Swiss National Science Foundation for financial support (Grants 2.256-0.81 and 2.209-0.81).

Registry No. ^{17}O, 13968-48-4; ^{99}Ru, 15411-62-8; $Ru(H_2O)_6^{2+}$, 30251-71-9; $Ru(H_2O)_6^{3+}$, 30251-72-0.

(30) Halle, B.; Wennerstroem, H. *J. Chem. Phys.* **1981**, *75*, 1928.
(31) Hertz, H. G. In "Progress in Nuclear Magnetic Resonance Spectroscopy"; Emsley, J. W.; Feeney, J.; Sutcliffe, L. H., Eds.; Pergamon Press: Oxford, 1967; Vol. 3, pp 159–230.
(32) Friedman, H. L. In "Protons and Ions Involved in Fast Dynamic Phenomena"; Laszlo, P., Ed.; Elsevier: Amsterdam, 1978; pp 27–41.
(33) Hertz, H. G. *Ber. Bunsenges. Phys. Chem.* **1973**, *77*, 531.
(34) Lucken, E. A. C. "Nuclear Quadrupole Coupling Constants"; Academic Press: New York, 1969.
(35) Fischer, H.; Tom, G. M.; Taube, H. *J. Am. Chem. Soc.* **1976**, *98*, 5512.
(36) Ulstrup, J. "Charge Transfer Processes in Condensed Media"; Springer-Verlag: West-Berlin, 1979; p 171.
(37) Sutin, N. *Prog. Inorg. Chem.* **1982**, *30*, 441; *Acc. Chem. Res.* **1982**, *15*, 275.
(38) $\nu_n \approx \nu_{in}\,[\Delta G^*_{in}/(\Delta G^*_{in} + \Delta G^*_{out})]^{1/2}$; $\nu_{in} = 2\nu_2\nu_3/(\nu_2 + \nu_3)$; ν_2 and ν_3 are the symmetric stretching frequencies (424 and 532 cm^{-1}).[11]
(39) $\Delta G^*_{in}(T) = \Delta G^*_{in}(\text{classical})(1/x)\tanh(x)$: $x = h\nu_{in}/(4k_BT)$; $\Delta S^*_{in}(T) = -\Delta G^*_{in}(T)(1 - 2x/\sinh(2x))/T$.[37]
(40) Hush, N. S. *Prog. Inorg. Chem.* **1967**, *8*, 391.